

Supplementary Information

Molecular locker probe enrichment of gene fusion variants from matched patient liquid biopsy specimens for magneto-bioelectrocatalytic nanosensing

Kevin M. Koo^{*ab}, Matt Trau^{*cd}

*^aThe University of Queensland Centre for Clinical Research (UQCCR), QLD 4029, Australia
Email: maisheng.koo@uqconnect.edu.au*

^bXING Applied Research & Assay Development (XARAD) Division, XING Technologies Pty Ltd, QLD 4073, Australia

*^cCentre for Personalized Nanomedicine, Australian Institute for Bioengineering and Nanotechnology (AIBN), The University of Queensland, QLD 4072, Australia
Email: m.trau@uq.edu.au*

^dSchool of Chemistry and Molecular Biosciences, The University of Queensland, QLD 4072, Australia

Table S1. Oligonucleotide sequences used in experiments. Locker probe sequences are underlined to indicate key fusion breakpoints in mutant variants and **highlighted** to indicate locked nucleic acid basemodifications. Key: Bio-C6-, Biotin modification with 6-carbon spacer.

Oligos	5'-Sequence-3'
<i>TMPRSS2</i> exons 1-2 locker probe	<u>CAATATG</u> *AC*CT*GCCG
<i>ERG</i> exons 3-4 locker probe	<u>GGCTTC</u> *CT*TG*ATATG
<i>ERG</i> exons 4-5 locker probe	<u>GGAGAGTTC</u> *CT*TG*AG
<i>ETV1</i> exons 3-4 locker probe	<u>ACCTGAG</u> *CT*TC*TGCA
T1E4 RPA Forward Primer	Bio-C6-CGGCAGGAAGCCTTATCA
T1E4 RPA Reverse Primer	GTTACATTCCATTTTGAT
T1E5 RPA Forward Primer	Bio-C6-CGGCAGGAAGCCTTATGA
T1E5 RPA Reverse Primer	CTGCTGGCACGATAACTC
T1ETV1 RPA Forward Primer	Bio-C6-CGGCAGGAAGCCTTATCT
T1ETV1 RPA Reverse Primer	TTTCTGAACATGGACTGT

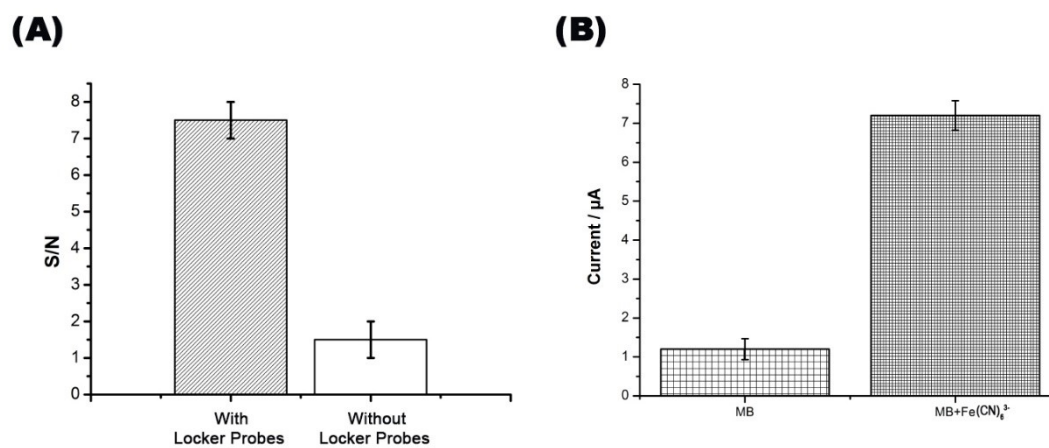


Fig. S1 Evaluation of the effects of locker probe enrichment and magneto-bioelectrocatalytic cycling on endpoint current measurements. (A) Current measurements in presence and absence of locker probe enrichment. (B) Current measurements using only DNA-intercalating MB or dual DNA-intercalating MB/freely diffusive $\text{Fe}(\text{CN})_6^{3-}$ bioelectrocatalytic cycling. Error bars represent standard deviation of three independent experiments ($n = 3$).

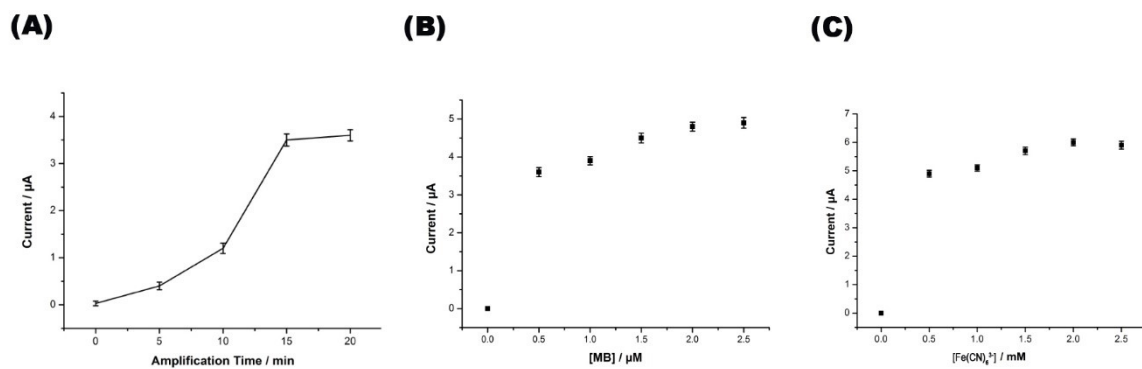


Fig. S2 Optimization of endpoint current signal. Current measurements at different (A) biotarget amplification times (B) MB concentrations and (C) $\text{Fe}(\text{CN})_6^{3-}$ concentrations. Error bars represent standard deviation of three independent experiments ($n = 3$).

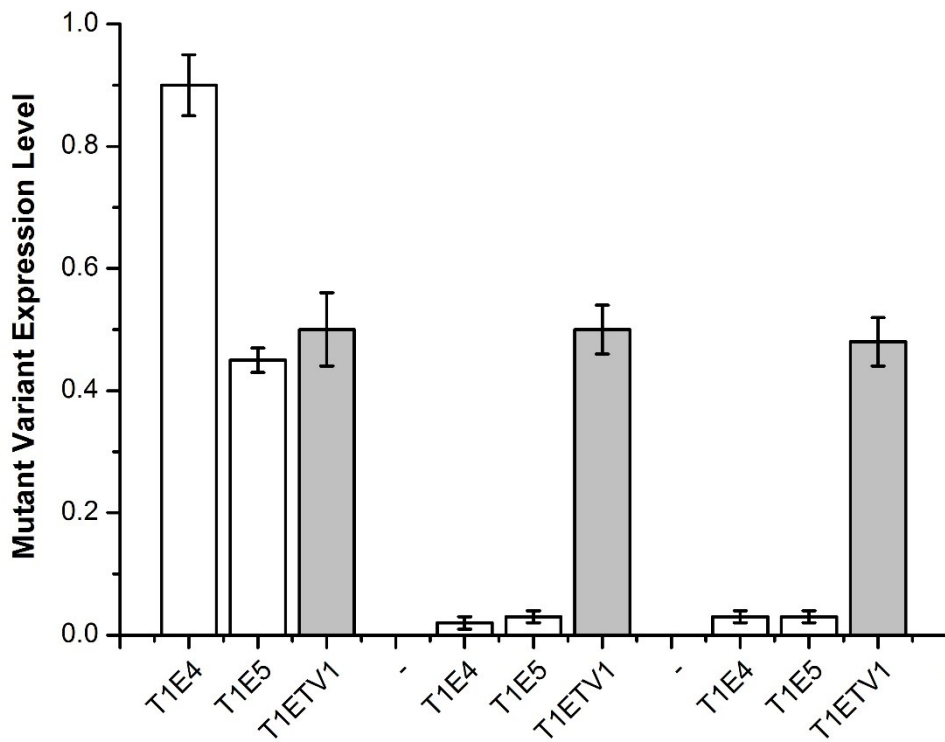


Fig. S3 Detection specificity for gene fusion mutant variants in cancer cell lines. specific T1ETV1 detection was shown by addition of T1ETV1 variant sequences (in grey) into all three cell lines. Error bars represent standard deviation of three independent experiments ($n = 3$).

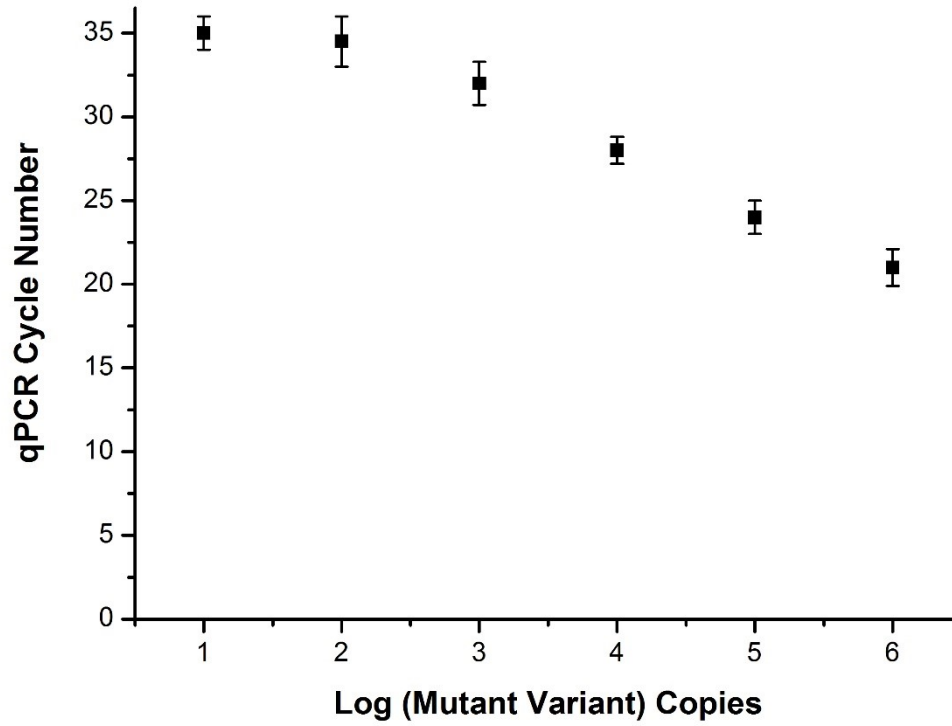


Fig. S4 Representative qPCR detection sensitivity limit and dynamic range for gene fusion mutant variants. Error bars represent standard deviations of triplicate independent measurements ($n = 3$).

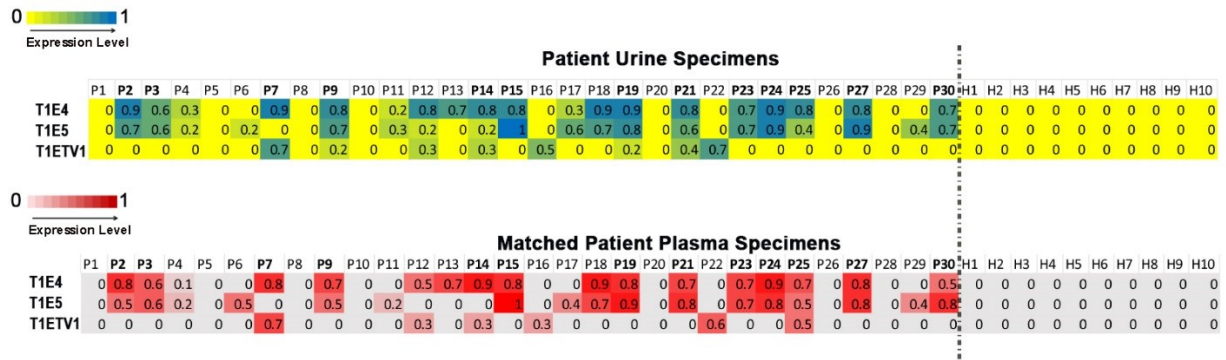


Fig. S5 Heat maps representing numerical data of mutant variant expression levels of T1E4, T1E5 and T1ETV1 in matched (top) urine and (bottom) plasma specimens. “P” denotes “Prostate Cancer Patient” and “H” denotes “Healthy Donor”. In bold are patients whose liquid biopsy specimens showed high expression for two or more of the gene fusion variant biotargets, and with poorer tumor grading outcomes.

Table S2. Tumor Gleason scores (GS) for study cohort of prostate cancer patients. In **bold** are patients whose liquid biopsy specimens showed high expression for two or more of the gene fusion variant biotargets. Key: GS<7, low-grade cancer; GS≥7, high-grade aggressive cancer.

	Gleason scoring
P1	GS<7
P2	GS≥7
P3	GS≥7
P4	GS<7
P5	GS<7
P6	GS<7
P7	GS≥7
P8	GS<7
P9	GS≥7
P10	GS<7
P11	GS<7
P12	GS<7
P13	GS≥7
P14	GS≥7
P15	GS≥7
P16	GS<7
P17	GS<7
P18	GS<7
P19	GS≥7
P20	GS≥7
P21	GS≥7
P22	GS≥7
P23	GS≥7
P24	GS≥7
P25	GS≥7
P26	GS<7
P27	GS≥7
P28	GS<7
P29	GS≥7
P30	GS≥7